

Oxide–Carbon Composites and Porous Metal Oxides Prepared via Water-Swellable Polymer Networks

Eli Ruckenstein* and Liang Hong

Department of Chemical Engineering of the State University of New York at Buffalo,
Buffalo, New York 14260

Received September 15, 1995. Revised Manuscript Received November 13, 1995⁸

Water-swellable polymer networks (WSPN) were employed as media for lodging metal nitrate salts or partially hydrolyzed tetraethyl orthosilicate (TEOS), which are precursors for inorganic oxides. The loading was achieved either via the polymerization of a suitable monomer and a cross-linker in an aqueous solution of the precursor or, in the case of TEOS, via the simultaneous polymerization of both monomers. The pyrolysis of the precursor-loaded network under N₂ flow generated interpenetrating networks of carbon and metal oxide. The combustion of the composite in air removed the carbon network and a porous metal oxide framework remained. On the basis of this methodology, a coating layer of C–SiO₂ composite was generated on a carbon-fiber, and porous powders of SiO₂, ZrO₂, MgO, and CuO–ZnO–Al₂O₃ oxide(s) were synthesized. It was found that the specific surface area of the oxides is affected by the nature of the WSPN. Two methodologies which lead to particles were developed. In one of them, sedimentation polymerization, large particles of about 1 mm size were obtained. In the other one, which starts from an emulsion of a water solution in an organic liquid (toluene, cyclohexane), micrometer size particles were prepared.

Introduction

Water-swellable polymer networks (WSPN) can function as water reservoirs because they can absorb large amounts of water. For this reason, they have been used in numerous applications.¹ The focus of the research was on the modification of their structure such as to promote or control the swelling capacity of the network, maintaining, of course, adequate mechanical properties.² With the exception of SiO₂,^{3–8} no attempts were, however, made to employ the WSPNs as reservoirs for lodging water-soluble inorganic salts and to use them to prepare and to affect the characteristics of the corresponding metal oxides. Since most of the polyelectrolyte polymers can contaminate the final oxide, the nonionic WSPNs will be preferred in what follows. Most of the hydrophilic functional groups present in the nonionic WSPNs possess a high affinity for inorganic cations; therefore, an inorganic salt will arrange in different ways in WSPNs that contain different functional groups. If an inorganic salt(s) loaded WSPN is subjected to pyrolysis, the porosity and the crystallinity of the inorganic oxide(s) generated will be determined to some extent by the nature of the WSPN.

In this paper, interpenetrating carbon–silica networks and porous metal oxide powders were prepared using WSPNs as the sources of carbon or as porogens.

In the preparation of the former material, the polymerization of the water-soluble monomers and the polycondensation of the hydrolyzed tetraethyl orthosilicate (TEOS, sol–gel process⁹) were carried out simultaneously in the same aqueous system; thus, an interpenetrating polymer–silica composite was generated. After pyrolysis under nitrogen, carbon–silica interpenetrating networks were obtained, which were transformed via combustion into porous silica. The idea to prepare interpenetrating networks of silica and organic polymers by the simultaneous polymerization of the corresponding monomers was reported by Novak et al.^{3–5} The emphasis in their work was on the preparation, via solution polymerization, of low-density monolithic composites of inorganic glasses and organic polymers, the goal being to eliminate the shrinkage problem associated with the sol–gel technique. In contrast, our main goal was to prepare particles. Two methodologies were developed in this respect. In one of them, sedimentation polymerization, large particles of about 1 mm were obtained. In the other one, which involved an emulsion of an aqueous solution in an organic liquid (toluene, cyclohexane), micrometer size particles were prepared.

In the preparation of porous metal oxides, a metal nitrate salt(s) was loaded into the WSPN either during the polymerization of the water-soluble monomer or via the swelling of a WSPN resin in an aqueous solution of the nitrate salt(s). During the pyrolysis, under a nitrogen atmosphere, of the nitrate salt(s) loaded WSPN, interpenetrating networks of carbon and metal oxide(s) were formed. When the carbon network was removed by combustion, a macroporous metal oxide framework was generated.

* To whom correspondence should be addressed.

Abstract published in *Advance ACS Abstracts*, January 1, 1996.

(1) Buchloz, F. L. *Chemtech*, **1994**, Sept, 38.

(2) *Polymers in Aqueous Media*; Glass, J. E., Ed.; American Chemical Society: Washington, DC, 1989.

(3) Novak, B. M.; Ellsworth, M.; Wallen, T.; Davies, C. *Am Chem. Soc., Polym. Prepr.* **1990**, 31, 698.

(4) Novak, B. M.; Davies, C. *Macromolecules* **1991**, 24, 5481.

(5) Ellsworth, M.; Novak, B. M. *J. Am. Chem. Soc.* **1991**, 113, 2756.

(6) Chujo, Y.; Matsuki, H.; Kure, S.; Saegusa, T.; Yazawa, T. *J. Chem. Soc., Chem. Commun.* **1994**, 635.

(7) Nakanishi, K.; Soga, N. *J. Non-Cryst. Solids* **1992**, 139, 1.

(8) Nakanishi, K.; Soga, N. *J. Am. Ceram. Soc.* **1991**, 74, 2518.

(9) Hench, L. L.; West, J. K. *Chem. Rev.* **1990**, 33.

The interpenetrating carbon-silica networks are employed in two applications: (1) the preparation of a silica with a controlled porosity; (2) the generation of a thin coating layer of interpenetrating carbon-silica composite on carbon fibers. A high-temperature treatment (which was not carried out by us) can convert the coating layer into a durable silicon carbide layer.

Mezo and macroporous metal oxide powders can find applications as metal oxide catalysts, catalyst supports, or adsorbents, because their porosity facilitates the mass transport of large molecular weight substrates. Three kinds of metal oxide powders were prepared: MgO , ZrO_2 and the tricomponent mixture of oxides $\text{CuO-ZnO-Al}_2\text{O}_3$. The investigation of the influence of the structure of WSPN on the surface area and structure of the metal oxide powders constitutes an additional goal of this paper.

Experimental Section

Chemicals. Most chemicals were purchased from Aldrich. Acrylamide (99%, AM), *N,N*-methylenebisacrylamide (99%, MBAM), 2-hydroxyethyl methacrylate (97%, HEMA), acrylic acid (99%, AC), poly(vinyl alcohol) (80% hydrolyzed, M_w = 9000–10000, PVA), glutaric dialdehyde (50 wt % in water, GDA), tetraethyl orthosilicate (99%, TEOS), magnesium nitrate hexahydrate (99%), zirconyl nitrate hydrate (99.99%), zinc nitrate hexahydrate (98%), and various solvents were used as received. Aluminum nitrate nonahydrate (98%) and copper nitrate trihydrate (98%) were purchased from Fisher Science Co., and the dispersant sorbitan monooleate (Span-80) from Fluka.

Preparation of Porous SiO_2 Spheres. *Sedimentation Polymerization.* In a 100 mL beaker, TEOS (10 g) and hydrochloric acid (6 mL, 1 N) were mixed by stirring until these two immiscible liquids became miscible because of the partial hydrolysis of TEOS. The aqueous solution was then mixed with another aqueous solution containing AM (7.14 g), MBAM (1.54 g), and $(\text{NH}_4)_2\text{S}_2\text{O}_8$ (0.1 g) in 15 mL of H_2O . The final aqueous solution was introduced dropwise as spheres of about 1.5 mm diameter with a syringe into a mineral oil heated at 95 °C located in a vertical cylindrical tube. The sedimentation residence time of the droplet in the column was about 8 s, time which in most cases was sufficiently long for polymerization to lead to the gelation of the droplets. Because of gelation, the droplets arrived at the bottom of the column, where they were kept for 2 h for the completion of the polymerization, did not coalesce. Spheres of about 1.5 mm diameter of interpenetrating P(AM-MBAM)- SiO_2 were thus prepared. For details about the sedimentation polymerization technique, one can see ref 10. The composite spheres placed in a ceramic sample boat were located in a tube furnace to carry out the pyrolysis and further the combustion in air. The final temperature, achieved via heating at a rate of about 10 °C/min, was 600 °C, temperature at which the spheres became white porous silica beads of about 0.8–1.0 mm in size.

Suspension Polymerization. In a 100 mL beaker, TEOS (10 g) and hydrochloric acid (10 mL, 0.1 N) were mixed by stirring until the two initially immiscible liquids became miscible because of the partial hydrolysis of TEOS. The aqueous solution was then mixed with another aqueous solution containing AM (7.14 g), MBAM (1.54 g), and $(\text{NH}_4)_2\text{S}_2\text{O}_8$ (6 mg) in 5 mL of H_2O . The obtained aqueous solution was dispersed via magnetic stirring in 30 mL of a toluene solution of Span-80 (1.2 g). The system was heated at 50 °C in an oil bath overnight to carry out the polymerization. The generated white granules were filtered and subjected to pyrolysis and combustion as in the previous procedure.

Dip-Coating of Carbon Fibers with a Thin Layer of C- SiO_2 Interpenetrating Composite. In a 100 mL beaker, TEOS (10 g) and an aqueous solution of PVA (10 g, 10 wt %

PVA), and HCl (1 mL, 1 N) were mixed with stirring until the two liquids became completely miscible. Then, short carbon fibers (~3 cm) were immersed into the aqueous solution, from which they were taken out after a few minutes. The coated carbon fibers were placed in a covered glass dish and cured at 60 °C overnight for the polycondensation of TEOS to occur. The carbon fibers thus treated were heated in a quartz tube at 600 °C under a N_2 flow for 1 h.

Preparation of the Porous ZrO_2 and MgO Particles.

In a 100 mL round bottom flask, a solution in 10 mL of water containing zirconyl nitrate hydrate (6.0 g), AM (7.14 g), MBAM (1.54 g), and the initiator $(\text{NH}_4)_2\text{S}_2\text{O}_8$ (5 mg) was introduced. Cyclohexane (30 mL) and Span-80 (1.5 g) were then added, the flask was sealed with a rubber septum and purged with a nitrogen flow for a few minutes. An emulsion of the aqueous solution in cyclohexane was generated by magnetic stirring. The polymerization was carried out by heating the flask in an oil bath (~65 °C) until the emulsion was transformed into a suspended powder (about 4 h). After cooling to room temperature, the powder was filtered and dried. The pyrolysis was carried out first in a quartz tube at 300 °C under a nitrogen flow until the complete decomposition of the nitrate salt (NO_2 was no longer eliminated). The black powder generated was then heated at 800 °C in air for 2 h to remove the carbon. A white ZrO_2 powder was thus obtained. Various water-soluble monomers and cross-linkers were employed. A similar procedure was used to prepare porous MgO powders from magnesium nitrate hexahydrate.

Preparation of $\text{CuO-ZnO-Al}_2\text{O}_3$ Tricomponent Metal Oxide Powders. The steps for the preparation of this tricomponent porous powder were as above, except the carbon removal by combustion which was carried out at 450 °C for 5 h.

A conventional coprecipitation procedure was used to prepare the reference sample free of macroporosity: An aqueous solution containing $\text{Zn}(\text{NO}_3)_2 \cdot 6\text{H}_2\text{O}$ (2.5 g, 8 mmol), $\text{Cu}(\text{NO}_3)_2 \cdot 3\text{H}_2\text{O}$ (1.25 g, 5 mmol) and $\text{Al}(\text{NO}_3)_3 \cdot 9\text{H}_2\text{O}$ (6 g, 16 mmol) in 15 mL of water was first prepared. To this solution a Na_2CO_3 solution (4 g in 15 mL of water) was added with mechanical stirring. The precipitate was washed several times with water and then dried in air. Its decomposition was conducted at 450 °C for 5 h.

Measurement of the Tap Density of ZrO_2 and MgO . Using a cylindrical tube, on which a given volume was marked by weighing pure water, a metal oxide powder was packed carefully with gentle shaking to avoid any dead space. The weight of the metal oxide was then divided by the volume.

Temperature-Programmed Reduction (TPR). Temperature-programmed reduction (TPR) was performed by heating the $\text{CuO-ZnO-Al}_2\text{O}_3$ from room temperature to 800 °C, at a rate of 17 °C/min, in a 4% H_2/Ar gas flow rate of 47 mL/min through a quartz tube of 2 mm inside diameter.

Instrumentation. The specific surface areas of metal oxide powders were measured by the BET method using a physical adsorption analyzer (2100E, Micromeritics). The infrared absorption spectra of the carbon- ZrO_2 composites were obtained with a Perkin-Elmer (1720) FT-IR instrument. The X-ray diffraction analysis of $\text{CuO-ZnO-Al}_2\text{O}_3$ powder was performed on a Nicolet X-ray diffraction equipment equipped with a $\text{Cu K}\alpha$ source, at 40 kV and 20 mA. Energy-dispersive spectroscopy (EDS) surface elemental analysis was performed using a PGT/IMIX field emission electron microscopy equipment. The porosities of the metal oxide particles were determined with a scanning electron microscope (SEM, Hitachi-800). Photographs were taken with a Sony MPI-DAGE video camera. The particle size distribution of ZrO_2 was determined using a HORIBA laser scattering particle size distribution analyzer (LA-900).

Results and Discussion

Combination of the Sol-Gel Process with Radical Polymerization in Aqueous Media. Unlike other metal alkyloxy salts, such as $\text{Al}(\text{OEt})_3$, tetraethyl orthosilicate (TEOS) and its derivatives hydrolyze and

Table 1. Porous Silica Substrates Prepared by the Pyrolysis of Interpenetrating WSPN-SiO₂ Composites^a

water-soluble monomer/cross-linker (mmol; g)	polymerization method	BET surface area of SiO ₂ (m ² /g)
AM-MBAM (100/10; 7.14/1.54)	sedimentation	450
AM-MBAM (100/10; 7.14/1.54)	suspension	85
HEMA-MBAM (57/5.7; 7.4/0.9)	suspension	555

^a TEOS (10 g) was used for the preparation of the samples listed in the table (see Experimental Section for details).

condense slowly in water or in a dilute acidic aqueous solution, at room temperature. When TEOS, which is immiscible with water, is mixed with a dilute acidic aqueous solution at room temperature, it experiences partial hydrolysis and transforms into water-soluble species. The gelation of the hydrolyzed TEOS usually needs several hours of heating. For this reason, one can combine in an aqueous system the sol-gel process of TEOS with the free radical polymerization of a water-soluble vinyl monomer. Since the two different type of polymerization occur simultaneously in a single-phase system, a composite of two interpenetrating polymer networks¹¹ is expected to be generated. To illustrate and investigate this bipolymerization, acrylamide (AM), and *N,N*-methylenebisacrylamide (MBAM) were used for the radical polymerization, and TEOS for the condensation polymerization. The sedimentation polymerization and the suspension polymerization described in the Experimental Section were employed to prepare the interpenetrating composites. The obtained P(AM-MBAM)-SiO₂ composites were then subjected to combustion to generate porous silica. The particles prepared via sedimentation polymerization had much higher surface areas than those obtained via suspension polymerization (Table 1). This indicates that the sedimentation polymerization results in a better interpenetration of the two networks. This probably happens because the high temperature (90–95 °C) of the heating medium promotes a rapid gelation of both polymers in the few seconds which the sedimentation lasts; the phase separation of the two polymers at lower temperatures which is caused by the different gelation rates is thus reduced to a minimum. The pore size distribution curve (Figure 1) of the silica spheres (Figure 2) shows that there are two kinds of pores; it is likely that the larger pores are due to the P(AM-MBAM) porogen. However, when HEMA-MBAM was used instead of AM-MBAM (Table 1), a much larger surface area was obtained via suspension polymerization than that via sedimentation polymerization. It appears that, because of its hydroxyl groups, the affinity of the HEMA polymer for the sol of hydrolyzed TEOS is stronger than that of the AM polymer, and it is likely that the more uniform the interpenetrating networks are, the larger the surface area generated. The sedimentation polymerization method was not successful in the case of HEMA-MBAM, probably because the extent of cogelation needed to avoid the coalescence of the droplets that arrived at the bottom of the sedimentation tube requires a longer time than the 8 s provided by our equipment; for this reason, the spheres that arrived at the bottom of the column coalesced before the complete polymerization occurred.

(11) *Interpenetrating Polymer Networks*; Klempner, D., Sperling, L. H., Utracki, L. A., Eds.; American Chemical Society: Washington, DC, 1994.

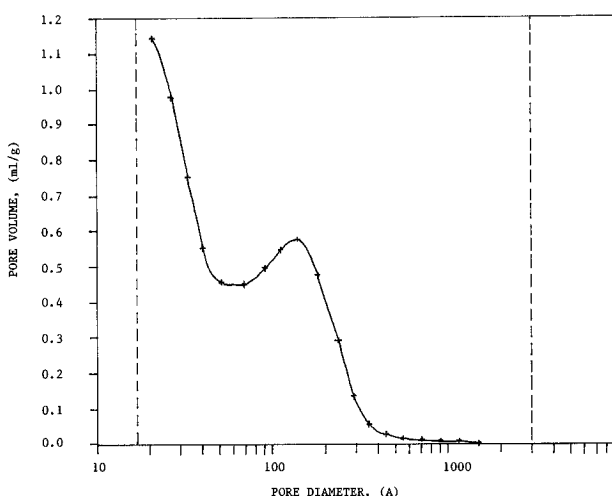


Figure 1. Pore-size distribution curve of the silica framework when AM-MBAM was used as a porogen and the sedimentation polymerization method was employed for polymerization.

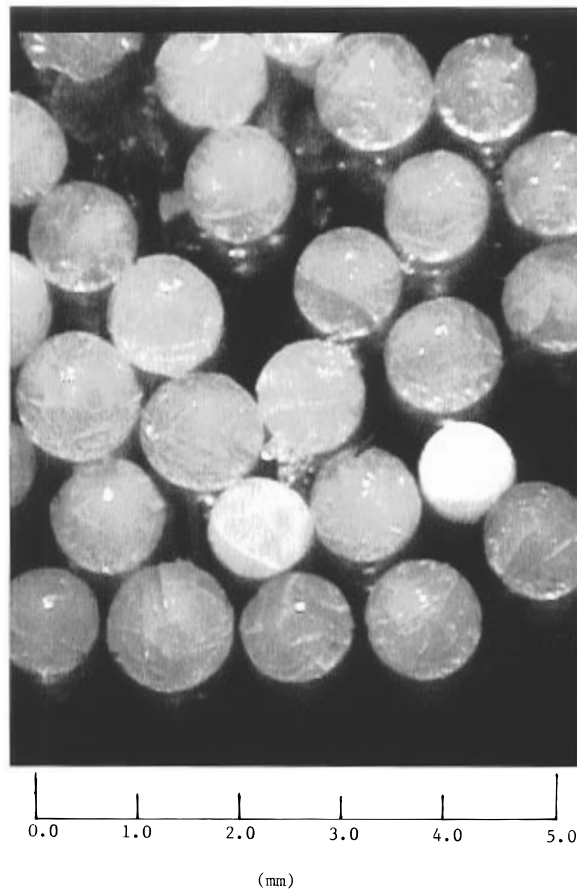


Figure 2. Silica beads obtained via sedimentation polymerization after removal of the AM-MBAM by pyrolysis and combustion.

In addition to the preparation of the porous SiO₂, another potential utility of this technique is to prepare a coating layer of carbon–silica composite on carbon fibers; this coating layer can be converted into a durable silicon carbide layer after high-temperature treatment.¹² To generate a coating layer of C–SiO₂ on the carbon fibers, a dilute acidic aqueous solution of PVA and partially hydrolyzed TEOS was prepared as a paint. Since the PVA used here contains 20 wt % polyvinylac-

(12) Kumada, M.; Tamao, K. *Adv. Organomet. Chem.* **1968**, 6, 19.

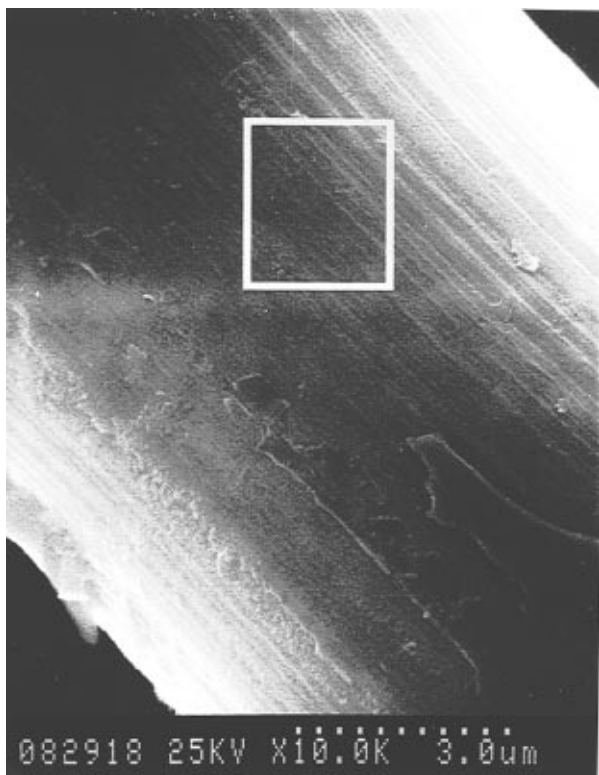


Figure 3. Scanning electron micrograph (SEM) of the surface of a C-SiO₂ coated carbon fiber.

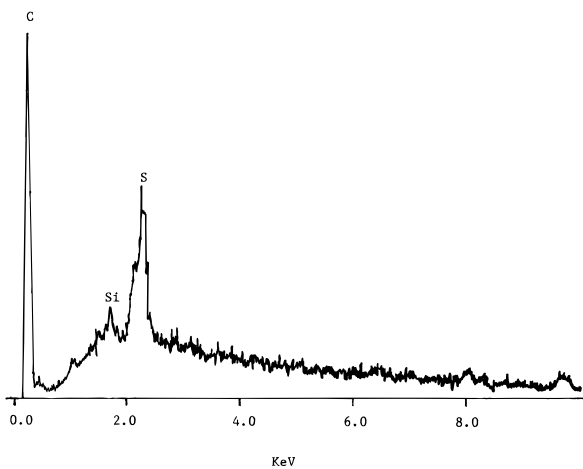


Figure 4. Energy-dispersive spectrum (EDS) of the microarea marked in Figure 3.

estate segments and 80 wt % poly(vinyl alcohol) segments, it behaves like a polymer surfactant; this enables the aqueous paint to spread over the surface of the carbon fiber. The aqueous coating layer was transformed into a semiinterpenetrating composite of PVA chains in a SiO₂ network after curing. When the coated carbon fiber was treated at 600 °C under a N₂ flow, the semiinterpenetrating composite of PVA in SiO₂ was converted into a carbon-silica composite. The EDS surface elemental analysis carried out on a microdomain (Figure 3) of the C-SiO₂ coated carbon fiber shows a weak Si absorption peak (Figure 4). The low intensity of the silica peak and the rather smooth SEM surface morphology (Figure 3) indicates that a thin C-SiO₂ composite layer was formed.

WSPN as Porogen. The influence of the structure of WSPN on the surface area and the internal void volume (which affects the value of the tap density) of

Table 2. Influence of the Structure of WSPN on the Surface Area and Internal Void Volume of Zirconium Oxide Powders^a

water-soluble monomer/cross-linker (mmol/g)	BET surface area of ZrO ₂ (m ² /g)	tap density (g/cm ³)
AM-MBAM (100/16; 7.14/2.48)	0.1	1.86
AM-MBAM (100/10; 7.14/1.54)	7.7	0.45
AM-MBAM (100/2; 7.14/0.3)	0.2	1.11
HEMA-MBAM (57/5.7; 7.4/0.9)	6.2	1.48
AC-MBAM (100/10; 7.2/1.54)	1.6	1.41

^a In all cases ZrO(NO₃)₂·3H₂O (6.0 g) and 10 mL of water were used together with the monomer and the cross-linker. The density of ZrO₂ is 5.89.

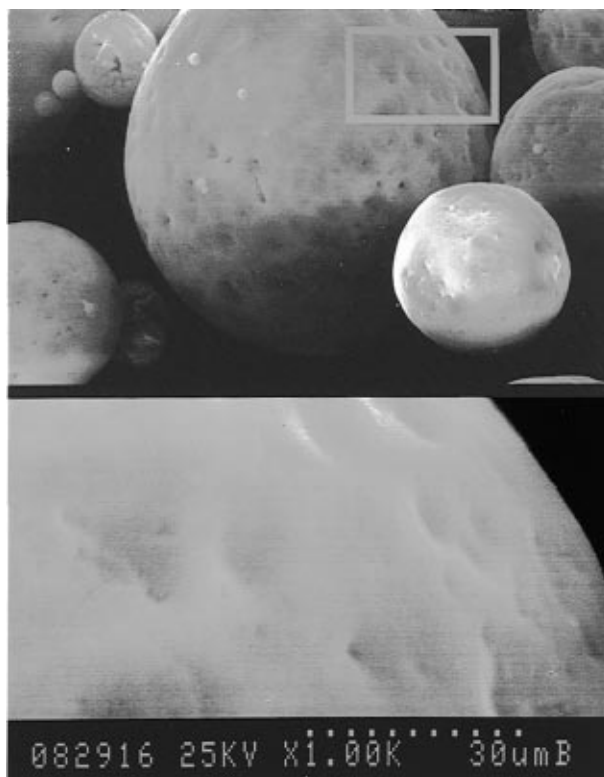


Figure 5. Scanning electron micrograph (SEM) of porous microspheres of ZrO₂ prepared using AM-MBAM as porogen.

the metal oxides was investigated by using various WSPN and by changing their cross-linking density. Table 2 lists the results for ZrO₂, and Figure 5 presents microspheres of ZrO₂. One can note that when AM-MBAM was used, the extent of cross-linking (determined by the weight ratio of AM to MBAM) affected profoundly the surface area and the internal void volume. There is an optimum cross-linking for which the surface area is maximum and the tap density minimum. A too high extent of cross-linking impedes completely the penetration of zirconyl nitrate in the polymer network, and this leads to small surface areas. A too low extent of cross-linking generates a loose polymer network, which, because of the freedom of the chains, leads to a nonuniform distribution of the precursor during pyrolysis. Consequently, after the carbon removal during combustion, the generated channels were nonuniformly distributed in the ZrO₂ particles. This leads to a low surface area and a high tap density. In addition, we found that the extent of cross-linking affects the size and the size distribution of the particles (Table 3). High extents of cross-linking result in small particle sizes, probably because less aggregation occurs.

Table 3. Effect of the Cross-Linking of WSPN on the Particle Size of Zirconium Oxide Powders

water-soluble monomer/cross-linker (mmol; g)	mean diameter (μm)	std dev (μm)
AM-MBAM (100/16; 7.14/2.48)	2.9	20.6
AM-MBAM (100/10; 7.14/1.54)	10.6	8.4
AM-MBAM (100/2; 7.14/0.3)	10.6	24.7

*The determinations were carried out using a suspension of the particles in an aqueous solution of Na_2HPO_4 (0.1 wt %).

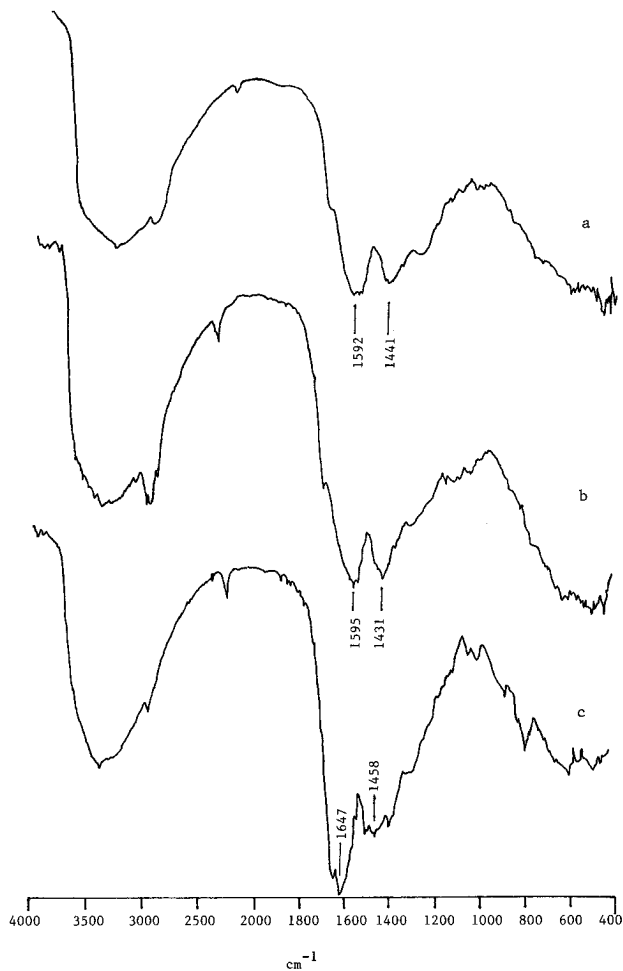


Figure 6. Infrared spectra of carbon– ZrO_2 composites based on three porogens: (a) AC–MBAM; (b) HEMA–MBAM; (c) AM–MBAM.

Two other WSPNs, HEMA–MBAM and AC–MBAM, were also used as porogens (Table 2). During preparation, we found that zirconyl nitrate salt (6.0 g) could not completely dissolve in 10 mL of water. When heated to 50 °C, a colloidal suspension was formed. However, as soon as either AM–MBAM or HEMA–MBAM was introduced, a clear solution was generated. This means that the water-soluble monomers AM and HEMA coordinate in some way the zirconyl cations. In contrast, AC–MBAM could not promote the solubility; the zirconyl nitrate remained as a colloidal dispersion, thus producing a less uniform distribution of the nitrate salt in the WSPN. This constitutes a possible explanation for the lower surface area of ZrO_2 prepared using AC–MBAM as porogen (Table 2).

The structure of the carbon network seems to have an influence on the internal void volume of ZrO_2 , since different WSPNs generate different structures of the carbon network and different porosities of the oxide. Indeed, the FT-IR spectra (Figure 6) of the carbon– ZrO_2

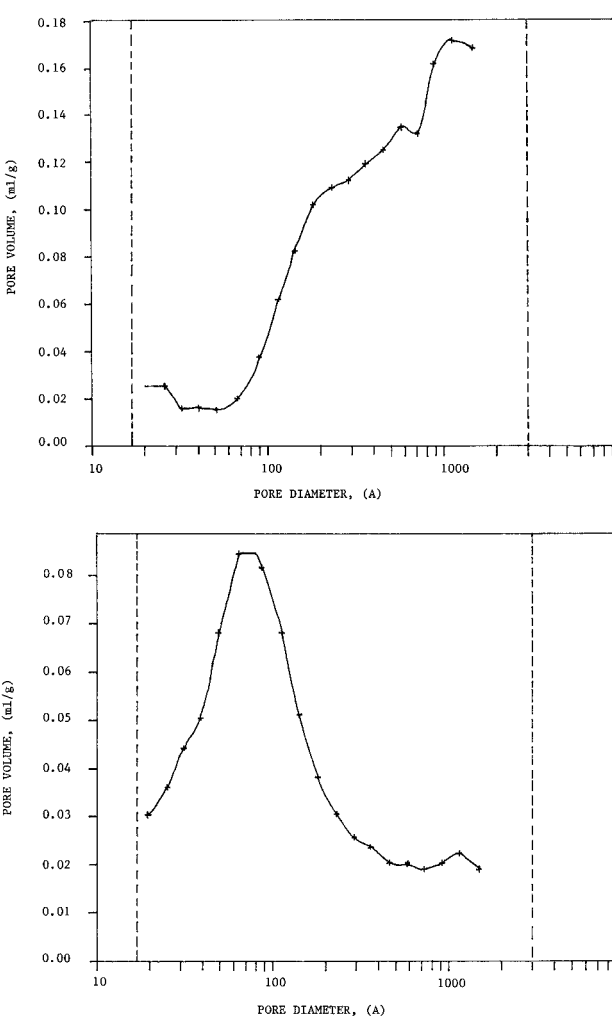


Figure 7. Pore-size distribution curves of the $\text{CuO-ZnO-Al}_2\text{O}_3$ based on (a, top) AM–MBAM or (b, bottom) PVA–DGA as porogen.

composites for the three WSPNs (listed in Table 2) show that the carbon networks generated by the pyrolysis of HEMA–MBAM and AC–MBAM have similar IR absorption bands. The carbon network generated via the pyrolysis of AM–MBAM exhibits, however, different IR absorption bands. The absorption bands at about 1590 cm^{-1} of the former can be attributed to the bending vibration modes of the polyaromatic frameworks;¹³ the band at 1647 cm^{-1} of the latter, which is close to the above values, can be also assigned to the bending vibration of a polyaromatic framework. Since a higher infrared frequency is likely associated with a larger three-dimensional polyaromatic network, the AM–MBAM network was transformed after pyrolysis into a larger polyaromatic framework than the other two WSPNs. Being more extended, the larger polyaromatic networks generate a large number of “microcracks” which are responsible for the higher porosity. These considerations explain why, for comparable conditions, the tap density of the ZrO_2 based on AM–MBAM is the lowest among the three, while the tap densities of the ZrO_2 based on HEMA–MBAM and on AC–MBAM are comparable (Table 2). One may note that the carbon network anchors only few oxygen-containing groups, because the characteristic carbon–oxygen single bond

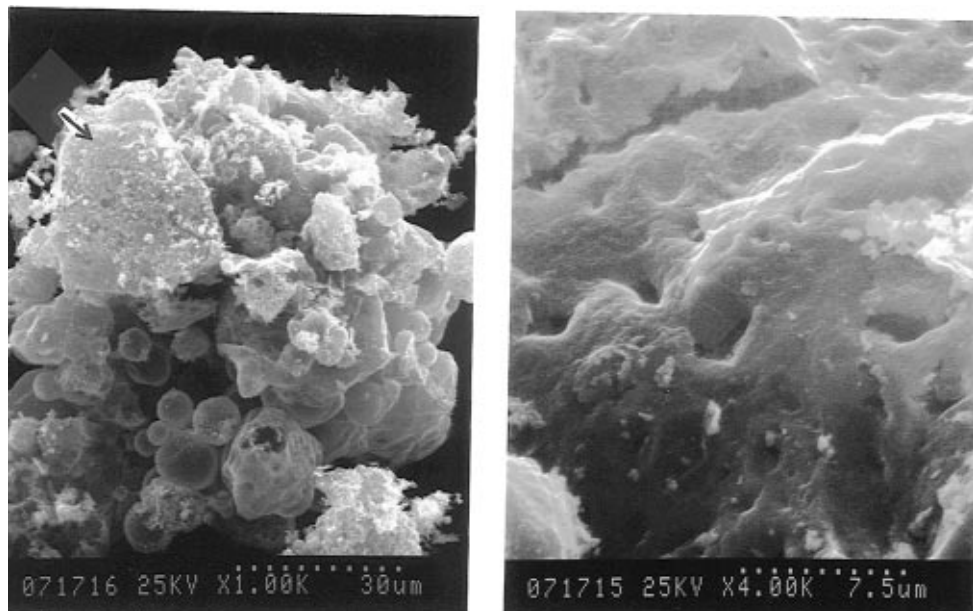


Figure 8. Scanning electron micrograph (SEM) of (a, left) $\text{CuO-ZnO-Al}_2\text{O}_3$ particles based on AM-MBAM as porogen. (b, right) Amplification of the region marked by an arrow in (a).

Table 4. Influence of the Structure of WSPN on the Surface Area and Internal Void Volume of Magnesium Oxide Powders^a

water-soluble monomer/cross-linker (mmol; g)	BET surface area MgO (m^2/g)	tap density (g/cm^3)
AM-MBAM (100/16; 7.14/2.48)	16.7	0.30
HEMA-MBAM (57/9; 7.4/1.4)	5.0	0.59
AC-MBAM (100/16; 7.2/2.48)	8.5	0.56
PVA-GDA ^b (109 ^c /17; 4.8/1.7)	12.1	0.49

^a The density of MgO is 3.58. ^b This sample was prepared by introducing 6.5 g of PVA-GDA powder into an aqueous solution of 6.5 g of $\text{Mg}(\text{NO}_3)_2 \cdot 6\text{H}_2\text{O}$ in 6 mL of water. ^c Millimoles of vinyl alcohol units.

stretching vibrations between 1200 and 1300 cm^{-1} are not present in the spectra. The bands at about 1440 cm^{-1} can be assigned to the carbon-hydrogen bending vibration mode of the aromatic structure.

Another application of the WSPNs as porogens is to the preparation of porous magnesium oxide via the decomposition of $\text{Mg}(\text{NO}_3)_2 \cdot 6\text{H}_2\text{O}$ loaded in various WSPNs (Table 4). Since $\text{Mg}(\text{NO}_3)_2 \cdot 6\text{H}_2\text{O}$ melts at 90 °C and decomposes at 130 °C, temperatures which are much lower than those needed to complete the pyrolysis of the four WSPN resins, the internal void volume of the obtained MgO powders depends less strongly on the carbon framework. However, the surface areas are still related to the nature of the WSPN. This happens because Mg^{2+} is a strong Lewis acid, and the Lewis basicity of the organic groups of the WSPNs follows the sequence amide > hydroxyl > carbonyl. One can therefore conclude that the affinity of the WSPNs for magnesium nitrate follows the sequence: AM-MBAM > PVA-GDA > AC-MBAM and HEMA-MBAM. The data regarding the surface area are consistent with this sequence. Indeed, the higher the cooperation between the functional groups of the WSPN and the metal ions, the more uniform the distribution of the latter and hence the larger the surface area.

Preparation of Porous Cu-Zn-Al Oxide Catalyst Using WSPNs as Porogens. Cu-Zn-Al oxide is an industrial catalyst used to synthesize methanol via

Table 5. Effect of WSPN on the Surface Area of Porous $\text{CuO-ZnO-Al}_2\text{O}_3$ Powders

water-soluble monomer/cross-linker (mmol; g)	nitrate salt hydrates of Cu/Zn/Al (mmol)	BET surface area (m^2/g)
precipitation method	9.5/20/6.5	65
AM-MBAM (100/10; 7.14/1.54)	9.5/20/6.5	33
PVA-GDA ^a (100 ^b /20; 4.4/2.0)	9.5/20/6.5	47

^a The nitrate salts were introduced into an aqueous solution of PVA and GDA in 64 mL of water; then the solution was suspended in 30 mL of toluene containing 3.0 g of Span-80. HCl (1.5 mL, 1 N) was then added to induce cross-linking. ^b Millimoles of vinyl alcohol units.

the reduction of CO with hydrogen.¹⁴ The conventional preparation is performed by the coprecipitation of the carbonate salts of the three components, and the micropores are generated by the elimination via heating of the carbon dioxide. In the present paper, the porosity is generated by the decomposition of the nitrate salts of the three metals loaded in a polymer network. Table 5 shows that the surface area of Cu-Zn-Al oxide (the molar ratios of the nitrate salt hydrates of $\text{Cu/Zn/Al} = 9.5/20/6.5$) prepared by coprecipitation is larger than those of the other two samples prepared by using WSPNs as porogens. Indeed, the pore size distribution curves (Figures 7) of the latter samples show that numerous macropores are present, their number being larger for the AM-MBAM porogen; the SEM micrographs (Figure 8) provide direct evidence.

In addition to functioning as a porogen, WSPN was found to be able to affect the structure of this tricomponent system. The temperature-programmed reduction experiments of the $\text{CuO-ZnO-Al}_2\text{O}_3$ (molar ratios of the nitrate salt hydrates of $\text{Cu/Zn/Al} = 5/8/16$, Table 6) provide information in this respect (Figure 9). In the sample prepared by the coprecipitation method there are two reduction peaks, one at 240 °C and the other one at about 540 °C. Only CuO can be reduced by H_2 at the above temperatures. The pure CuO has a single peak at 250 °C. The presence of the other oxides

Table 6. Effect of WSPN on the Surface Area of Porous CuO-ZnO-Al₂O₃ Powders

water-soluble monomer/cross-linker (mmol; g)	nitrate salt hydrates of Cu/Zn/Al (mmol)	BET surface area(m ² /g)
precipitation method	5/8/16	98
AM-MBAM (100/10; 7.14/1.54)	5/8/16	52
HEMA-MBAM (57/5.7; 7.4/0.9)	5/8/16	46
PVA-GDA ^a (150 ^b /18; 6.6/1.8)	5/8/16	52

^a The PVA-GDA powder (8.4 g) was introduced into an aqueous solution of the nitrates in 10 mL of water. ^b Millimoles of vinyl alcohol units.

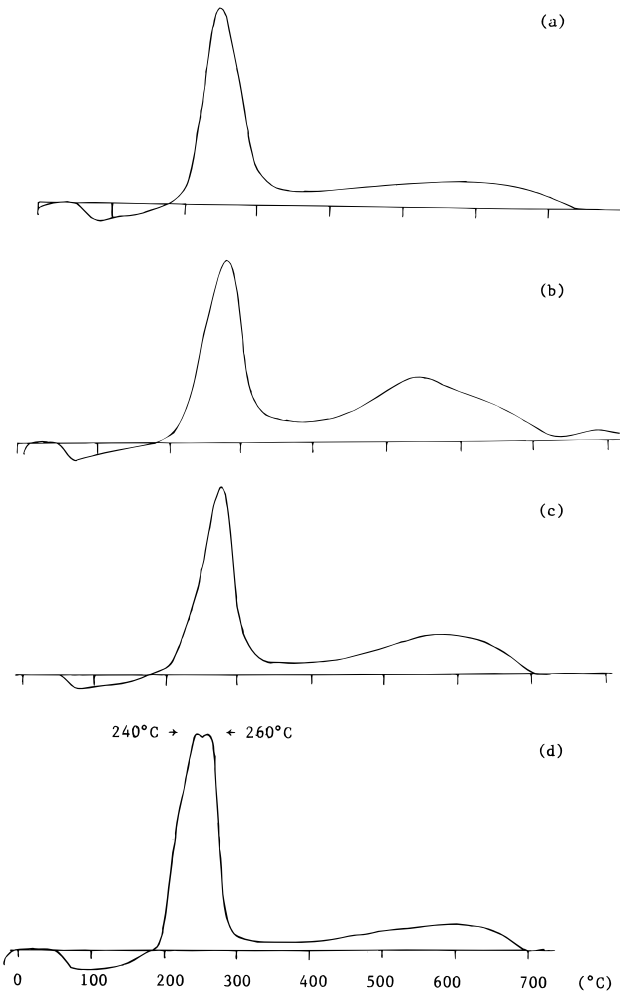


Figure 9. Temperature-programmed reduction (TPR) curves of CuO-ZnO-Al₂O₃ specimens: (a) coprecipitation method; (b) AM-MBAM as porogen; (c) HEMA-MBAM as porogen; (d) PVA-GDA as porogen.

changes the environment of CuO, but for an isotropic mixture a single peak is still expected to occur at a different temperature (for the above composition the peak is at 220 °C¹⁵). The presence of several peaks indicates that several chemical surroundings are present and hence that the system is heterogeneous. The area of the first peak indicates that about 87% of CuO was reduced at the lower temperature. The sample based on the AM-MBAM network contains about 59% CuO reduced at the lower temperature, while the sample based on the HEMA-MBAM network contains about 67% CuO reduced at the lower temperature. The

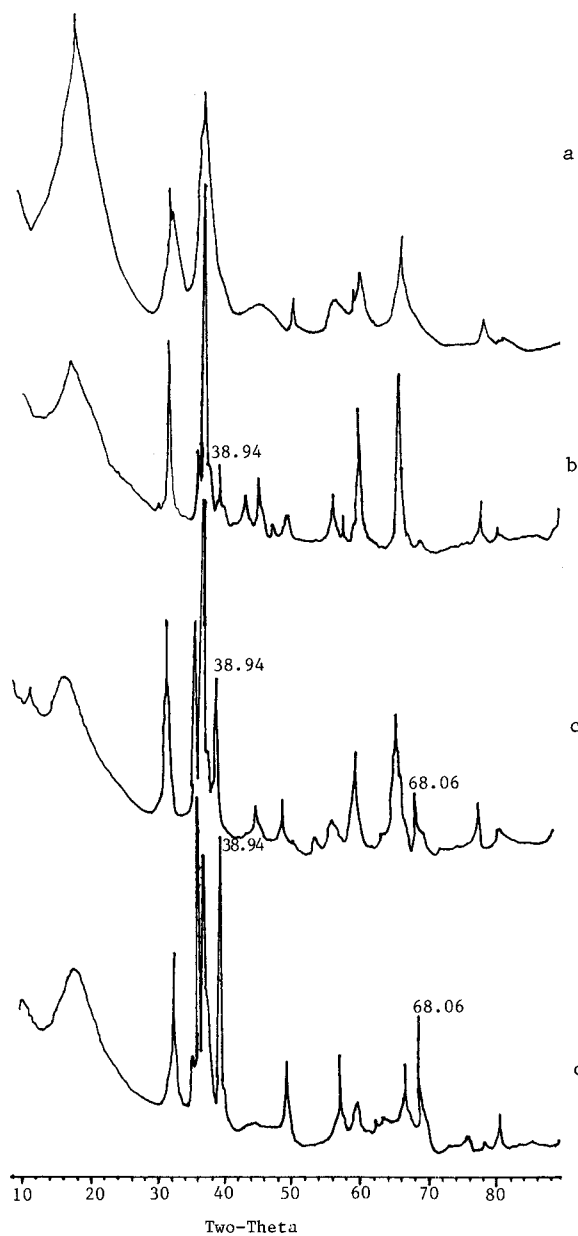


Figure 10. X-ray powder diffractions of the CuO-ZnO-Al₂O₃ specimens: (a) coprecipitation method; (b) AM-MBAM as porogen; (c) HEMA-MBAM as porogen and (d) PVA-GDA as porogen.

sample based on PVA-GDA exhibits three reduction peaks. The peaks at the lower temperatures are almost overlapped (240 and 260 °C) and represent more than 86% of CuO. The X-rays powder diffraction experiments of four samples (Figure 10) show that the relative intensities of the peaks at $2\theta = 38.9$ and 68.1° , which can be assigned to CuO,¹⁶ is in the sequence PVA-GDA > HEMA-MBAM > AM-MBAM. The TPR peak at 240 °C is the same for all four specimens. It is probably due to CuO which has in its environment ZnO and Al₂O₃, since pattern a of the XRD (Figure 10) does not indicate the presence of pure CuO. However, the TPR peak at 260 °C, which appears in curve d (Figure 9), can be attributed to pure CuO since the XRD pattern d (Figure 10) clearly indicates its presence. The lower XRD intensities for pure CuO in the patterns b and c suggest that smaller amounts of pure CuO are present

in those specimens (they overlap with the peak at 240 °C). The high-temperature TPR peak can be attributed to CuO belonging to an alloy of the three oxides. One can conclude that WSPN determines to some extent the phase structure of the multicomponent metal oxides. It appears that the arrangement of metal nitrate salts in a given WSPN is affected by the interactions between the functional groups of the network and the ions of the salts.

Conclusion

A water-swellable polymer network (WSPN) was employed as a source of carbon or as a porogen to prepare oxide–carbon composites and porous oxides from inorganic salt precursors. The procedure consisted of three steps: first, the inorganic precursor(s) was introduced into the WSPN; then, the precursor-loaded WSPN was subjected to pyrolysis under an inert atmosphere to generate a carbon–metal oxide composite; finally, the combustion in air removed the carbon network, in most cases. The WSPN is employed for several purposes: (1) it allows the preparation of interpenetrating carbon–silica composites, (2) it generates mesopores (10^2 – 10^3 Å) into the metal oxide matrix,

and (3) it affects the structure of the metal oxide. Regarding the first purpose, the sol–gel process of tetraethyl orthosilicate (TEOS) and the free radical polymerization of a water-soluble monomer and cross-linker were conducted simultaneously. This interpenetrating system was also used to prepare a coating layer of C–SiO₂ composite on carbon fibers. Regarding the second purpose, porous SiO₂, ZrO₂, MgO, and Cu–Zn–Al oxides were prepared as examples. We found that the surface area of the porous oxides was affected by the nature of the WSPN, via its extent of cross-linking and its pendant functional groups. Regarding the third purpose, the X-ray diffraction and temperature-programmed reduction (TPR) have revealed the phase changes in the porous CuO–ZnO–Al₂O₃ induced by various WSPNs.

Acknowledgment. This work was supported by the National Science Foundations. We are indebted to DuPont Central Research and Development Experimental Station for performing the pore size distribution measurements.

CM950431U